

RESEARCH ARTICLE | AUGUST 18 2022

On the conduction mechanism in compositionally graded AlGaN

Shashwat Rathkanthiwar ; Pegah Bagheri; Dolar Khachariya; ... et. al

 Check for updates

Appl. Phys. Lett. 121, 072106 (2022)

<https://doi.org/10.1063/5.0100756>



View
Online



Export
Citation

CrossMark

Articles You May Be Interested In

Effect of dopant compensation on the temperature dependence of the transport properties in p-type monocrystalline silicon

Journal of Applied Physics (February 2014)

Charge carrier dynamics and recombination in graded band gap $\text{CuIn}_{1-x}\text{Ga}_x\text{Se}_2$ polycrystalline thin-film photovoltaic solar cell absorbers

Journal of Applied Physics (October 2013)

Chemical composition and strength of dolomite geopolymers composites

AIP Conference Proceedings (September 2017)



Time to get excited.
Lock-in Amplifiers – from DC to 8.5 GHz



[Find out more](#)

 Zurich
Instruments

On the conduction mechanism in compositionally graded AlGaN

Cite as: Appl. Phys. Lett. **121**, 072106 (2022); doi: [10.1063/5.0100756](https://doi.org/10.1063/5.0100756)

Submitted: 26 May 2022 · Accepted: 31 July 2022 ·

Published Online: 18 August 2022



View Online



Export Citation



CrossMark

Shashwat Rathkanthiwar,^{1,a)} Pegah Bagheri,¹ Dolar Khachariya,² Ji Hyun Kim,¹ Yasutomo Kajikawa,³ Pramod Reddy,² Seiji Mita,² Ronny Kirste,² Baxter Moody,² Ramon Collazo,¹ and Zlatko Sitar^{1,2} 

AFFILIATIONS

¹Department of Materials Science and Engineering, North Carolina State University, Raleigh, North Carolina 27695-7919, USA

²Adroit Materials, Inc., 2054 Kildaire Farm Rd., Cary, North Carolina 27518, USA

³Interdisciplinary Faculty of Science and Engineering, Shimane University, Matsue 690-8504, Japan

^{a)}Author to whom correspondence should be addressed: srathka@ncsu.edu

ABSTRACT

A two-band transport model is proposed to explain electrical conduction in graded aluminum gallium nitride layers, where the free hole conduction in the valence band is favored at high temperatures and hopping conduction in the impurity band dominates at low temperatures. The model simultaneously explains the significantly lowered activation energy for p-type conduction (~ 10 meV), a nearly constant sheet conductivity at lower temperatures (200–330 K), and the anomalous reversal of the Hall coefficient caused by the negative sign of the Hall scattering factor in the hopping conduction process. A comparison between the uniform and graded samples suggests that compositional grading significantly enhances the probability of phonon-assisted hopping transitions between the Mg atoms.

Published under an exclusive license by AIP Publishing. <https://doi.org/10.1063/5.0100756>

Aluminum gallium nitride (AlGaN) has been identified as one of the essential semiconductor material systems for modern-day power electronics¹ and optoelectronics.² To achieve high performance in these devices, it is necessary to realize low-resistivity n- and p-type AlGaN layers. While Si/Ge doping has been demonstrated to be effective in achieving n-type AlGaN films across a range of doping levels and compositions,³ efficient p-type doping remains a significant challenge throughout the AlGaN compositional range. Mg is the most explored p-type dopant in AlGaN. The relatively high ionization energy that increases from 260 to 780 meV (Ref. 4) with an increase in Al-content is the fundamental bottleneck for achieving a high bulk hole concentration via Mg doping. Only a small fraction of the Mg atoms ionize at room temperature (RT) to generate free holes and contribute to p-type conductivity. The majority of Mg atoms remains in a neutral configuration, and to conduct, they must undergo a multi-phonon hopping process involving tunneling.⁵ This tunneling is associated with the overlap of the atomic wavefunctions of initial and final atomic configurations.⁶ Neumann pointed out that the effect of impurity band conduction becomes more pronounced with the increase in acceptor ionization energy.⁷ A signature of hopping conduction has indeed been observed in p-type GaN,^{8–10} Al-rich AlGaN,^{11–13} and SiC¹⁴ at relatively high doping levels $>10^{19}$ cm⁻³, and in other material systems, such as p-type GaAs,¹⁵ InP,¹⁶ and InSb,¹⁷ at low doping

levels in the range of 10¹⁷ cm⁻³. In most cases, the onset of impurity band conduction was observed at low temperatures where the free hole conduction is suppressed.

Compositionally graded AlGaN films have been shown to exhibit a significant improvement in p-conductivity with a drastically reduced thermal activation as compared to bulk GaN and AlGaN films.^{18–24} The case of Mg-doped, compositionally graded AlGaN is distinct in the sense that the bandgap and the Mg acceptor ionization energy scale with the Al content. Also, the compositional change along the thickness in a c-axis oriented AlGaN film is expected to lead to the presence of a volumetric polarization charge.²⁵ The sign of the charge is determined by the polar orientation of the film and the direction of grading, where a metal-polar (nitrogen-polar) compositionally graded AlGaN layer grown with decreasing (increasing) Al composition leads to a negative volumetric polarization charge. Although this charge is bound and does not contribute to the electrical conductivity directly, it has been proposed that the electric field produced by this charge is large enough to attract carriers from available sources of charge (surface and remote dopants) such that a three-dimensional (3D) mobile hole slab will be formed.^{18,25} Despite the prediction of a 3D hole slab in the undoped linearly graded layers,²⁵ all reported temperature-dependent Hall-effect studies of compositionally graded p-AlGaN layers have relied on intentional Mg doping.^{18–22,24} Interestingly, the

Mg doping concentration in these studies exceeded the estimated volumetric polarization charge density by several times. It has been suggested that the need for intentional Mg doping arises due to the presence of deep-level traps that localize holes and due to the limited propensity of the surface to provide remote acceptor states.^{18,26} Additionally, it has been hypothesized that the polarization field in the graded layer assists in the ionization of Mg acceptors.¹⁸ To this end, the room temperature hole concentrations were reported to reasonably match the estimated volumetric polarization charge density.^{18–21}

These hypotheses have attracted several questions regarding the hole generation and conduction mechanism in the graded AlGaN structures. For a Mg-doped, compositionally graded AlGaN layer, the position of the valence band maxima and the position of the Mg acceptor level relative to the valence band maxima vary as a function of the Al content. The impact of these variations and the impact of the polarization field in the graded layer on the electronic orbital overlap, between which the carriers transfer, have not been studied and need a comprehensive investigation.

The purpose of this Letter is to build an understanding of the conduction mechanism in Mg-doped, compositionally graded AlGaN films. We discuss in detail the temperature-dependent electrical resistivity and Hall coefficient in these films. We demonstrate a two-band transport mechanism where free hole conduction in the valence band and hopping conduction in the impurity band dominate p-conduction at high and low temperatures, respectively.

Graded AlGaN structures [Fig. 1(a)] were grown in a vertical, cold-walled, low-pressure, RF-heated metalorganic chemical vapor deposition (MOCVD) reactor at a growth temperature of 1300 K and total pressure of 20 Torr. Trimethylaluminum (TMA), triethylgallium (TEG), ammonia (NH₃), and bis(cyclopentadienyl) magnesium (Cp₂Mg) were used as the precursors for Al, Ga, N, and Mg, respectively. A 400-nm thick AlN layer was first grown on a c-plane sapphire substrate, followed by unintentionally doped 750-nm thick Al_{0.50}Ga_{0.50}N and 50-nm thick Al_{0.40}Ga_{0.40}N layers. Next, a 200-nm thick compositionally graded layer was grown at a high V/III ratio of 8000 and Mg doping of 10¹⁹ cm⁻³. The Al-mole fraction was decreased linearly from 0.40 to 0.10. A 3-nm thick p-GaN was grown on the top of this structure to act as a contact layer for Hall-effect measurements. Another sample consisting of 200-nm thick Mg-doped p-GaN was grown under similar growth conditions and was used as a reference sample for the Hall studies.

The linearity of the composition gradient was confirmed using secondary ion mass spectroscopy (SIMS) and electron dispersive spectroscopy in a transmission electron microscope (TEM), FEI T-30. The hydrogen, oxygen, and carbon impurity concentrations were determined using SIMS. The surface morphology of the films was inspected using an Asylum Research MFP-3D atomic force microscope (AFM) in a tapping mode. The photoluminescence (PL) spectroscopy was performed at room temperature (RT) using a 190 nm ArF laser with a power density of 1 mW/cm². Ni/Au (20/40 nm) contacts were e-beam deposited in the van der Pauw geometry on 1 × 1 cm² samples for electrical measurements. The contacts were annealed at 875 K for 10 min under O₂ ambient for Ohmic contact formation. Temperature-dependent resistivity and Hall measurements were performed in a temperature range of 200–700 K using a Lake Shore 8400 series AC/DC Hall measurement system. For an accurate determination of the Hall coefficients, a 1.18 T AC magnetic field was used with a lock-in amplifier.

The graded AlGaN structure [Fig. 1(a)] exhibited a smooth surface morphology as shown in Fig. 1(b) with an RMS roughness of 1.6 nm. The hydrogen concentration in the as-grown film was found to be 2 × 10¹⁸ cm⁻³, five times lower than the Mg concentration. Recent Mg-doped AlGaN reports have also demonstrated lower hydrogen levels (compared to GaN) in the as-grown films, pointing to a lower concentration of the Mg–H complex.^{12,13} Oxygen, carbon, and nitrogen vacancies act as compensating donors in p-type AlGaN.²⁷ Oxygen and carbon concentrations were below the SIMS detection limit <10¹⁷ cm⁻³. Figure 1(c) shows the room-temperature PL spectrum for the graded AlGaN structure. The peak position at 3.6 eV corresponds to the band edge of the end composition (10% Al) of the graded AlGaN layer. Expectedly, due to the high V/III ratio used for the growth of the graded layer, no carbon-related or nitrogen-vacancy-related peaks were observed.²⁸

Figures 2(a) and 2(b) show the measured temperature-dependent resistivity (ρ) and Hall coefficient (R_H) for the graded AlGaN structure. This is representative data from eight 1 cm² samples. The eight samples showed a ~10% variation in ρ and a ~15% variation in R_H , albeit a very similar temperature dependence, which is the focus of this Letter. The graded AlGaN exhibited a nearly constant resistivity from 200 to 320 K. Above 320 K, the resistivity showed a 50 meV activation energy. This is in contrast to the reference GaN sample grown under the same growth conditions, which showed an activation energy of ~120 meV [Fig. 3(a)]. For the reference GaN sample, the sign of R_H [Fig. 3(b)] is positive across the entire temperature range and its

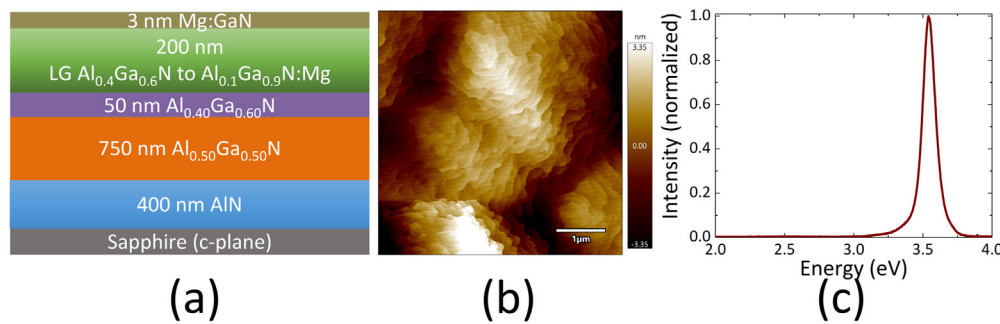


FIG. 1. (a) Schematic of the epitaxial stack. (b) AFM topography revealing a smooth surface. (c) RT PL spectrum obtained from the structure (a).

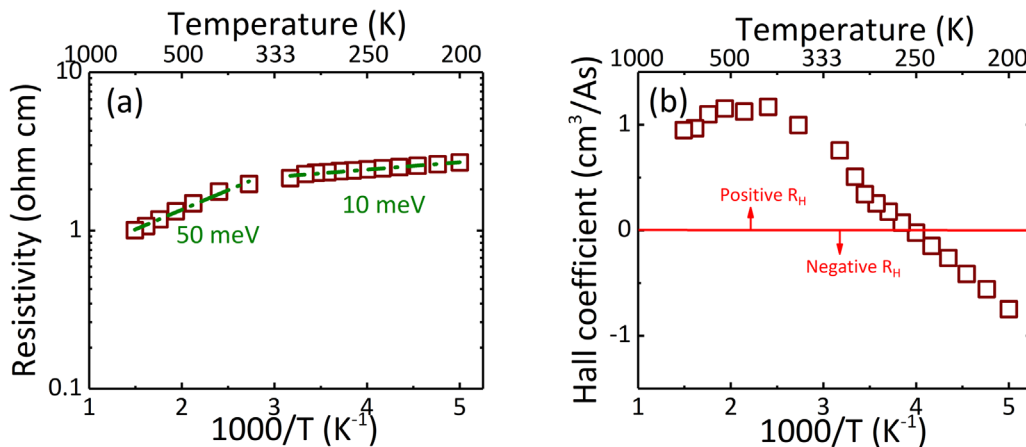


FIG. 2. Temperature-dependent (a) resistivity and (b) Hall coefficient for the Mg-doped graded AlGaN structure.

magnitude shows an exponential increase as the temperature is lowered. This is indicative of an exponential decrease in the hole concentration, p ($R_H = A/qp$), where A is the Hall scattering factor and q is elementary charge as the temperature is lowered, which is a typical carrier freeze out behavior for p-GaN films due to the high Mg ionization energy. For the graded AlGaN structure, R_H exhibits much smaller values than for the GaN control sample [Fig. 2(b)]. For instance, at room temperature, R_H measured $0.5 \text{ cm}^3/\text{As}$ as compared to $\sim 10 \text{ cm}^3/\text{As}$ for GaN. For an assumption of pure valence band transport, this value correlates with a free hole concentration of $1.3 \times 10^{19} \text{ cm}^{-3}$. At higher temperatures, R_H varies in the range of $0.5\text{--}1.1 \text{ cm}^3/\text{As}$. Surprisingly, as the temperature is lowered, R_H exhibits a transition in the sign from positive to negative. To examine the possibility of conduction in the layers underneath the graded layer, measurements were performed on another sample grown without Mg doping. The undoped sample was found to be highly resistive until 100 V , thus ruling out a parasitic conduction path.

The reduced thermal dependence of resistivity [Fig. 2(a)] for the Mg-doped graded AlGaN structure (compared to the reference GaN)

and the anomalous reversal of the sign of R_H [Fig. 2(b)] are characteristic features of the impurity band hopping conduction.^{5,6,29,30} The Hall effect associated with the hopping motion of carriers differs qualitatively from the quasi-free motion of itinerant carriers, such as free holes in the valence band. According to the theory of Holstein and Friedman, to define the Hall effect in such systems, one needs to consider the occurrence of coincidence events involving an initially occupied site and at least two final sites.⁶ They found Hall mobility (μ_{Hall}) to be extremely sensitive to the geometric arrangement of the sites involved in the hopping process. Thus, the local atomic geometry (relative orientations and symmetry) and the nature (s-like, p-like, bonding, and antibonding) of local electronic orbitals between which the carrier transfers play significant roles in governing μ_{Hall} .^{29–31}

An important finding of Holstein's theory is concerned with the sign of R_H . As the sign of the Hall effect depends upon the product of electronic transfer integrals, which link the local orbitals about the closed loop, the author concluded that the sign of the Hall coefficient is the same (different) for holes and electrons for processes involving an odd (even) number of orbitals.²⁹ The observation of a negative R_H

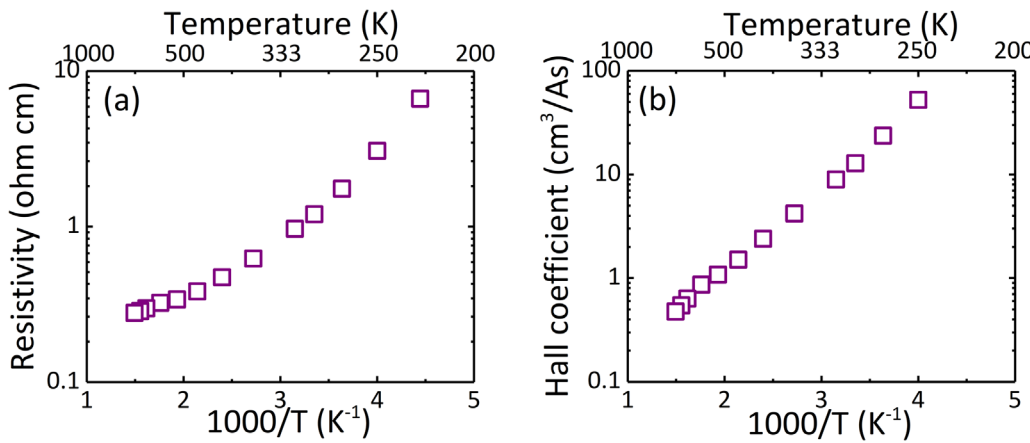


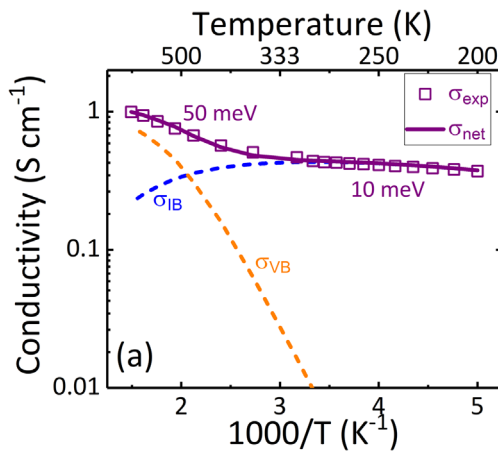
FIG. 3. Temperature-dependent (a) resistivity and (b) Hall coefficient for the Mg-doped GaN reference sample.

at low temperatures in Fig. 2(b) confirms a negative Hall scattering factor for hopping conduction (A_{hop}) in graded AlGaN, in agreement with Kajikawa's finding of the negative sign of A_{hop} in p-GaN.³² Recently, the sign of A_{hop} was also reported to be negative for p-SiC.¹⁴ Another important feature of Friedman and Holstein's theory is that the activation energy of μ_{Hall} for hopping conduction is one-third that of drift mobility (μ_{drift}).⁶ This means that μ_{Hall} can have values much larger than μ_{drift} . This has an important consequence on the magnitude of A_{hop} , the ratio of Hall and drift mobilities, which can have values far exceeding $A_{\text{VB}} \approx 1$. This means that for the same carrier concentration, hopping conduction will produce a much higher R_{H} as compared to the free hole conduction in the valence band. Additionally, A_{hop} varies as a function of temperature. For the case of nearest-neighbor hopping conduction, A_{hop} is given by³¹

$$A_{\text{hop}} = \frac{k_B T}{J_{\text{hop}}} \exp\left(\frac{K_{\text{NNH}} T_{\text{hop}}}{T}\right), \quad (1)$$

where K_{NNH} , J_{hop} , and T_{hop} are considered as fitting parameters in the model discussed below.

To understand the results in Fig. 2, we consider an analytical model based on two-band conduction consisting of free hole conduction in the valence band and hopping conduction in the impurity band. We follow Kajikawa's methodology to fit the data.^{32,33} Figures 4(a) and 4(b) show the comparison of the experimentally measured and modeled values of effective conductivity (σ_{net}) and effective Hall coefficient ($R_{\text{H}}^{\text{net}}$) with the respective contributions from the two conduction mechanisms. The net conductivity, $\sigma_{\text{net}} = \sigma_{\text{VB}} + \sigma_{\text{hop}}$, where $\sigma_{\text{VB}} = q p_{\text{VB}} \mu_{\text{VB}}$ and $\sigma_{\text{hop}} = q p_{\text{hop}} \mu_{\text{hop}}$. p_{VB} is the concentration of holes in the valence band calculated using charge neutrality and semiconductor statistics. p_{hop} is the concentration of neutral (un-ionized) Mg atoms. The valence band mobility (μ_{VB}) was calculated for an average Al composition of 25% within the relaxation-time approximation by using Matthiessen's rule for scattering due to non-polar optical phonons, acoustic phonons, and ionized impurities.³⁴ The material parameters involved were interpolated from the values of GaN and AlN.^{35,36} μ_{hop} for nearest neighbor hopping conduction is given by³¹



$$\mu_{\text{hop}} = \mu_{\text{hop}0} \left(\frac{T_{\text{hop}}}{T}\right)^{3/2} \exp\left(-\frac{T_{\text{hop}}}{T}\right), \quad (2)$$

where $\mu_{\text{hop}0}$ and T_{hop} were considered as fitting parameters in this model.

Modeling shown in Fig. 4(a) reveals that σ_{VB} and σ_{hop} dominate at high and low temperatures, respectively. Above 320 K, their opposite temperature dependences cumulatively result in σ_{net} with a much reduced thermal dependency of ~ 50 meV, which is much lower than the true Mg ionization energy of >200 meV. This mechanism differs from the previous hypothesis¹⁸ that suggested that the polarization field in the compositionally graded layer assists in the ionization of Mg acceptors.

The Hall coefficients for the valence band (R_{H}^{VB}) and hopping ($R_{\text{H}}^{\text{hop}}$) conductions are given by

$$R_{\text{H}}^{\text{VB}} = \frac{A_{\text{VB}}}{q p_{\text{VB}}}, \quad (3)$$

$$R_{\text{H}}^{\text{hop}} = \frac{A_{\text{hop}}}{q p_{\text{hop}}}. \quad (4)$$

The contribution of these two Hall coefficients to the combined conduction $R_{\text{H}}^{\text{net}}$ depends on the respective conductivities of the two conduction mechanisms,

$$R_{\text{H}}^{\text{net}} = R_{\text{H}}^{\text{VB}} \left(\frac{\sigma_{\text{VB}}}{\sigma_{\text{net}}}\right)^2 + R_{\text{H}}^{\text{hop}} \left(\frac{\sigma_{\text{hop}}}{\sigma_{\text{net}}}\right)^2. \quad (5)$$

For valence band transport, $A_{\text{VB}} \approx 1$; therefore, R_{H}^{VB} is always positive, whereas the negative sign of A_{hop} leads to a negative $R_{\text{H}}^{\text{hop}}$. It is to be noted that R_{H}^{VB} is inversely proportional to p_{VB} . Thus, R_{H}^{VB} is large at low temperatures. However, as seen in Fig. 4(a), as the temperature is lowered and Mg ionization decreases, the dominating transport transitions from the valence band to hopping conduction. In other words, at low temperatures, $\sigma_{\text{VB}} \ll \sigma_{\text{net}}$, and thus, $R_{\text{H}}^{\text{net}} \cong R_{\text{H}}^{\text{hop}}$. Therefore, $R_{\text{H}}^{\text{net}}$ transitions from a positive value at high temperatures to a negative value at low temperatures. At this point, it is important

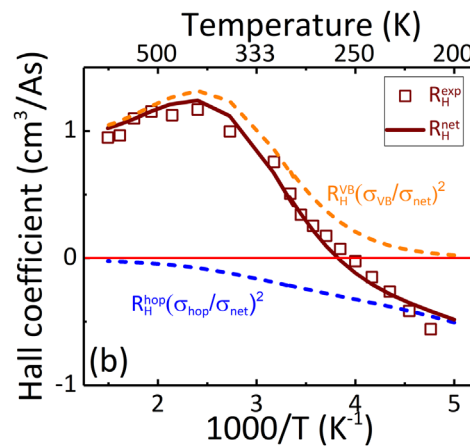


FIG. 4. Comparison of experimentally measured and analytically modeled values of (a) conductivity and (b) Hall coefficient for the Mg-doped graded AlGaN structure. The modeled values of contributions from valence band conduction and hopping conduction are also shown. Note: The values of parameters, Mg ionization energy, $\mu_{\text{hop}0}$, T_{hop} , K_{NNH} , and J_{hop} were 270 meV (for an average Al composition of 25%), 0.3 cm²/V s, 450 K, 1.2, and 600 meV, respectively.

to highlight that the hopping conduction has a large influence on the values of ρ and R_H even at high temperatures. While the former is attributed to the fact that hopping conduction is temperature-activated, the latter is a consequence of the negative sign and large magnitude of the A_{hop} coefficient. The observation of enhanced hopping conductivity in this study suggests that the compositional grading significantly enhances the probability of phonon-assisted transitions between Mg atoms. The two-band transport mechanism discussed here also explains the results by Yasuda *et al.*²⁴ who observed a similar flip in sign of carriers (Hall coefficient) from p-type (positive) to n-type (negative) in a Mg-doped graded AlGaN structure at low temperatures.

It is important to note that, often, the contextual analysis of resistivity and Hall effect data is not straightforward, especially in p-type wide bandgap semiconductors where the acceptors are deep and valence band conduction may be limited due to a low population of ionized acceptors. For instance, if the impurity band conduction is neglected, the activation energy for the hole concentration can appear to be systematically lower than the true ionization energy of the acceptor. In extreme cases, this can lead to the wrong conclusion that the acceptor has a nearly vanishing ionization energy. Obviously, a correct interpretation of the experimental data is only possible by extending the measurements to a wider temperature range. Impurity band conduction can only be ruled out for the cases where the theoretical temperature dependence of the free hole concentration (p_{VB}) and mobility (μ_{VB}) yield a good simultaneous fit to the hole concentration extracted from $p = 1/qR_H$ and mobility extracted from $\mu = \rho R_H$, with fitting parameters of the acceptor concentration, compensating donor concentration, and acceptor ionization energy. Here, p_{VB} is estimated by considering semiconductor statistics and charge neutrality,³⁷ and μ_{VB} is estimated by considering various scattering mechanisms.³⁷ Deviations from the ideal valence band behavior should be analyzed using the two-band model demonstrated in this work.

In summary, we studied the carrier transport mechanisms in Mg-doped, compositionally graded (40%–10% Al) AlGaN films with metal polarity. The apparently anomalous results deviating from classical semiconductor physics were analyzed based on a two-band transport mechanism consisting of free hole valence band and hopping impurity band conduction. Free hole conduction in the valence band and hopping conduction in the impurity band dominated at high and low temperatures, respectively. Based on these data, we propose that the compositional grading significantly enhances the probability of phonon-assisted hopping transitions between Mg atoms.

The authors gratefully acknowledge funding in part from AFOSR (Nos. FA9550-17-1-0225, FA9550-19-1-0114, and FA9550-19-1-0358), NSF (Nos. ECCS-1610992, ECCS-1508854, ECCS-1916800, and ECCS-1653383), and ARO (No. W911NF-16-C-0101).

AUTHOR DECLARATIONS

Conflict of Interest

The authors have no conflicts to disclose.

Author Contributions

Shashwat Rathkanthiwar: Conceptualization (equal); Data curation (lead); Formal analysis (lead); Investigation (lead); Methodology

(lead); Writing – original draft (lead); Writing – review and editing (lead). **Ramon Collazo:** Conceptualization (equal); Funding acquisition (equal); Project administration (equal); Resources (equal); Validation (equal); Visualization (equal); Writing – review and editing (equal). **Zlatko Sitar:** Conceptualization (equal); Funding acquisition (equal); Project administration (equal); Resources (equal); Validation (equal); Visualization (equal); Writing – review and editing (equal). **Pegah Bagheri:** Investigation (supporting). **Dolar Khachariya:** Investigation (supporting). **Ji Hyun Kim:** Investigation (supporting). **Yasutomo Kajikawa:** Data curation (equal); Software (equal). **Pramod Reddy:** Conceptualization (equal); Formal analysis (supporting). **Seiji Mita:** Investigation (supporting); Resources (equal). **Ronny Kirste:** Project administration (equal); Resources (equal); Validation (equal). **Baxter Moody:** Conceptualization (supporting); Visualization (supporting); Writing – review and editing (supporting).

DATA AVAILABILITY

The data that support the findings of this study are available from the corresponding author upon reasonable request.

REFERENCES

1. Y. Tsao, S. Chowdhury, M. A. Hollis, D. Jena, N. M. Johnson, K. A. Jones, R. J. Kaplar, S. Rajan, C. G. Van de Walle, E. Bellotti, C. L. Chua, R. Collazo, M. E. Coltrin, J. A. Cooper, K. R. Evans, S. Graham, T. A. Grotjohn, E. R. Heller, M. Higashiwaki, M. S. Islam, P. W. Juodawlkis, M. A. Khan, A. D. Koehler, J. H. Leach, U. K. Mishra, R. J. Nemanich, R. C. N. Pilawa-Podgurski, J. B. Shealy, Z. Sitar, M. J. Tadjer, A. F. Witulski, M. Wraback, and J. A. Simmons, *Adv. Electron. Mater.* **4**, 1600501 (2018).
2. H. Amano, R. Collazo, C. D. Santi, S. Einfeldt, M. Funato, J. Glaab, S. Hagedorn, A. Hirano, H. Hirayama, R. Ishii, Y. Kashima, Y. Kawakami, R. Kirste, M. Kneissl, R. Martin, F. Mehnke, M. Meneghini, A. Ougazzaden, P. J. Parbrook, S. Rajan, P. Reddy, F. Römer, J. Ruschel, B. Sarkar, F. Scholz, L. J. Schowalter, P. Shields, Z. Sitar, L. Sulmoni, T. Wang, T. Wernicke, M. Weyers, B. Witzigmann, Y.-R. Wu, T. Wunderer, and Y. Zhang, *J. Phys. D* **53**, 503001 (2020).
3. S. Washiyama, K. J. Mirrieles, P. Bagheri, J. N. Baker, J.-H. Kim, Q. Guo, R. Kirste, Y. Guan, M. H. Breckenridge, A. J. Klump, P. Reddy, S. Mita, D. L. Irving, R. Collazo, and Z. Sitar, *Appl. Phys. Lett.* **118**, 042102 (2021).
4. J. L. Lyons, A. Janotti, and C. G. Van de Walle, *J. Appl. Phys.* **115**, 012014 (2014).
5. E. F. Schubert, *Doping in III-V Semiconductors* (Cambridge University Press, 2015).
6. L. Friedman and T. Holstein, *Ann. Phys.* **21**, 494 (1963).
7. H. Neumann, *Cryst. Res. Technol.* **23**, 1377 (1988).
8. B. Gunning, J. Lowder, M. Moseley, and W. Alan Doolittle, *Appl. Phys. Lett.* **101**, 082106 (2012).
9. P. Kozodoy, H. Xing, S. P. DenBaars, U. K. Mishra, A. Saxler, R. Perrin, S. Elhamri, and W. C. Mitchel, *J. Appl. Phys.* **87**, 1832 (2000).
10. D. Lancefield and H. Eshghi, *J. Phys.* **13**, 8939 (2001).
11. T. Kinoshita, T. Obata, H. Yanagi, and S. Inoue, *Appl. Phys. Lett.* **102**, 012105 (2013).
12. P. Bagheri, A. Klump, S. Washiyama, M. Hayden Breckenridge, J. H. Kim, Y. Guan, D. Khachariya, C. Quinones-García, B. Sarkar, S. Rathkanthiwar, P. Reddy, S. Mita, R. Kirste, R. Collazo, and Z. Sitar, *Appl. Phys. Lett.* **120**, 082102 (2022).
13. A. Jadhav, P. Bagheri, A. Klump, D. Khachariya, S. Mita, P. Reddy, S. Rathkanthiwar, R. Kirste, R. Collazo, Z. Sitar, and B. Sarkar, *Semicond. Sci. Technol.* **37**, 015003 (2022).
14. Y. Kajikawa, *J. Electron. Mater.* **50**, 1247 (2021).
15. A. Wolos, M. Piersa, G. Strzelecka, K. P. Korona, A. Hruban, and M. Kaminska, *Phys. Status Solidi C* **6**, 2769 (2009).
16. M. Benzaquen, B. Belache, and C. Blaauw, *Phys. Rev. B* **46**, 6732 (1992).

¹⁷S. A. Obukhov, *AIP Adv.* **2**, 022116 (2012).

¹⁸J. Simon, V. Protasenko, C. Lian, H. Xing, and D. Jena, *Science* **327**, 60 (2010).

¹⁹A. Kalra, S. Rathkanthiwar, R. Muralidharan, S. Raghavan, and D. N. Nath, *IEEE Photonics Technol. Lett.* **31**, 1237 (2019).

²⁰L. Zhang, K. Ding, J. C. Yan, J. X. Wang, Y. P. Zeng, T. B. Wei, Y. Y. Li, B. J. Sun, R. F. Duan, and J. M. Li, *Appl. Phys. Lett.* **97**, 062103 (2010).

²¹R. Dalmau and B. Moody, *ECS Trans.* **86**, 31 (2018).

²²L. Yan, Y. Zhang, X. Han, G. Deng, P. Li, Y. Yu, L. Chen, X. Li, and J. Song, *Appl. Phys. Lett.* **112**, 182104 (2018).

²³T. Yasuda, K. Yagi, T. Suzuki, T. Nakashima, M. Watanabe, T. Takeuchi, M. Iwaya, S. Kamiyama, and I. Akasaki, *Jpn. J. Appl. Phys.* **52**, 08JJ05 (2013).

²⁴T. Yasuda, T. Takeuchi, M. Iwaya, S. Kamiyama, I. Akasaki, and H. Amano, *Appl. Phys. Express* **10**, 025502 (2017).

²⁵C. Wood and D. Jena, *Polarization Effects in Semiconductors* (Springer, 2008).

²⁶D. Jena, J. Simon, A. K. Wang, Y. Cao, K. Goodman, J. Verma, S. Ganguly, G. Li, K. Karda, V. Protasenko, C. Lian, T. Kosel, P. Fay, and H. Xing, *Phys. Status Solidi A* **208**, 1511 (2011).

²⁷T. Narita, K. Tomita, Y. Tokuda, T. Kogiso, M. Horita, and T. Kachi, *J. Appl. Phys.* **124**, 215701 (2018).

²⁸A. Klump, M. Hoffmann, F. Kaess, J. Tweedie, P. Reddy, R. Kirste, Z. Sitar, and R. Collazo, *J. Appl. Phys.* **127**, 045702 (2020).

²⁹T. Holstein, *Philos. Mag.* **27**, 225 (1973).

³⁰D. Emin, *Philos. Mag.* **35**, 1189 (1977).

³¹C. Chien and C. Westgate, *The Hall Effect and Its Applications* (Springer Science & Business Media, 2013).

³²Y. Kajikawa, *Phys. Status Solidi C* **14**, 1600129 (2017).

³³Y. Kajikawa, *Phys. Status Solidi C* **13**, 387 (2016).

³⁴T. Narita, K. Tomita, K. Kataoka, Y. Tokuda, T. Kogiso, H. Yoshida, N. Ikarashi, K. Iwata, M. Nagao, N. Sawada, M. Horita, J. Suda, and T. Kachi, *Jpn. J. Appl. Phys.* **59**, SA0804 (2020).

³⁵D. C. Look, J. Sizelove, S. Keller, Y. Wu, U. Mishra, and S. DenBaars, *Solid State Commun.* **102**, 297 (1997).

³⁶H. Morkoç, *Nitride Semiconductors and Devices* (Springer, 1999), pp. 8–44.

³⁷K. Seeger, *Semiconductor Physics: An Introduction*, 9th ed. (Springer, 2004).